Proceedings of The Institute of Acoustics

QUARTER WAVELENGTH MATCHING OF AIR-BACKED PIEZOELECTRIC DISCS TO A WATER LOAD

N.G. PACE and P.D. THORNE*

School of Physics, University of Bath.
* Now at I.O.S., Taunton.

INTRODUCTION

The efficiency of underwater sound transducers can be obtained by directly measuring both the electrical power delivered to the transducer and the resulting acoustic power present in the water. Alternatively, the efficiency can sometimes be obtained from electrical admittance measurements at the transducer terminals when the transducer is loaded in turn by water and by air. If the radiation impedance can be reduced to zero by replacing the water load by an air load then the efficiency may be obtained from the diameters of the motional admittance circles for the two loadings. However, replacing the water load by air does not always result in a zero radiation impedance. In fact when face plates are employed to increase the bandwidth of the transducer when operating in water, the radiation impedance with an air load, at the frequency for resonance with water loading, is considerably higher than with a water load.

It is the purpose of this paper to explore the possibility of calculating transducer efficiency from electrical admittance measurements. To this end the input electrical admittance of an air-backed piezoelectric disc fitted with a perspex face plate was measured as a function of frequency for both air and water loading for a number of values of face plate thickness. In addition the efficiency of the transducers were obtained using a self-reciprocity technique (2).

An analysis of the transducer using transmission line equivalent circuits (1) for the piezoelectric disc and the face plate (see Figure 1) shows that the form of the electrical input conductance depends on the value of $(\rho c)_{FP}/(\rho c)_{load}$. For small values of $(\rho c)_{FP}/(\rho c)_{load}$ such as obtain for perspex and water, the electrical input conductance shows a single broad peak whilst for large values the conductance shows two well separated narrower peaks. The ratio $(\rho c)_{FP}/(\rho c)_{load}$ becomes large for air loading regardless of the parameters of the face plate. The two conductance peaks occur at the frequencies f_1 and f_2 ($f_1 < f_2$) at which the input susceptance is zero. An examination of the expressions for the input conductance for air loading at frequencies f_1 and f_2 shows that the electrical losses R_e (see Figure 1) are approximately

$$R_e = \left[\left(1 + \frac{(\rho c)_{FP} \tan \alpha'_{1,2}}{(\rho c)_c \tan (\alpha_o)_{1,2}}\right)^2 \Big/ G_{1,2}\right] - \frac{A(\rho c)_{load}}{4\phi^2} \tan^2 \alpha'_{1,2} \qquad (1)$$

where $\alpha'_{1,2} = \frac{\pi}{2}(f_{1,2}/f')$ and $G_{1,2}$ is the input conductance measured at either f_1 or f_2. Unless $f_{1,2}$ is very close to f' the second term may be neglected. Thus a knowledge of the height of the conductance peaks for air loading and G' the maximum conductance for water loading which occurs close to f', allows in principle the calculation of the efficiency

$$\eta = 1 - R_e G' . \qquad (2)$$

The values of f_1 and f_2 depend on f' , the frequency for which the face plate is quarter-wavelength as shown in Figure 2. A usual requirement is that the face plate should be quarter-wavelength at f'_o , this being termed the water matched case. In this matched situation the f_1 and f_2 conductance peaks measured when air loaded are symmetrically spaced either side of f'_o. If the face plate quarter-wavelength frequency f' is much less than f'_o then the f_1 peak occurs close to f' whilst the f_2 peak occurs close to f'_o. On the other hand if the face plate quarter-wavelength frequency f' is much greater than f'_o then the f_1 peak occurs close to f'_o and the f_2 peak close to f'.

EXPERIMENTAL RESULTS AND DISCUSSION

A transducer was constructed as shown in Figure 3, the different face plate thicknesses listed in Table 1 being obtained by machining. Relevant parameters of the transducer are given in Figure 1.

The measured electrical input conductances are shown in Figure 4 together with the theoretical curves obtained from the transmission line model for both air and water loadings. The electrical losses used in the model calculations were determined by achieving a close fit between the experimental and theoretical conductance curves for the water loaded case. Losses determined in this manner are denoted by L_2 and are shown in Table 2. The experimentally determined positions of the conductance peaks for air loading are indicated on Figure 2, the error bars reflecting the uncertainty in the uniformity of face plate thicknesses.

As can be seen from the theoretical curves in Figure 4 the Q-factor for the two conductance peaks for any one of the air loaded transducers are markedly different except when the face plate quarter-wavelength frequency is close to f_o'. The height of the conductance peaks obtained experimentally and thus the losses calculated using equation (1) (denoted by L_1 and shown in Table 2) is dependant on the relative magnitude of the theoretical conductance peak bandwidth $(BW)_{1,2}$ and the spread $(2\Delta f_{1,2})$ in conductance peak position $f_{1,2}$ due to non-uniformity of face plate thickness. Table 1 lists the spread in the expected position of the conductance peaks together with the half-power bandwidth $(BW)_{1,2}$ of the conductance peaks obtained from the transmission line model. If the ratio $(BW)_{1,2}/2\Delta f_{1,2})$ is significantly larger than unity then the estimate of losses using equation (1) is expected to be better than if the ratio is small.

Estimates of the efficiency of the transducers using either the losses L_1 or L_2 in equation (2) are shown in Figure 5 together with the efficiencies measured using the self-reciprocity technique (2). The three points which are apparently under-estimates of efficiency correspond to the three cases for which estimates of losses L_1 from conductance peaks are expected to be poor due to the particularly low values of the ratio $(BW)/2\Delta f)$ as shown in Table 1.

In order to ensure the estimate of efficiency using the electrical losses obtained for air loaded conductance measurements is as good as the best achieved in this work, the ratio $(BW)/2\Delta f)$ should be at least five. Applying this figure to the case of the "matched to water" face plate thickness, a uniformity of face plate thickness of ± 0.001 mm is required.

CONCLUSIONS

The results presented here suggest that the electrical losses for use in efficiency calculations of simple disc transducers broad-banded by use of face plates may be obtained from air loaded electrical input conductance measurements provided the uniformity of the face plate thickness is better than about 0.3%.

REFERENCES

1. KOSSOFF G. The effects of backing and matching on the performance of piezo electric ceramic transducers. IEEE Trans. Sonics and Ultrasonics, SU-13, 20-30, (1966)

2. The self-reciprocity technique for efficiency measurement is a diffraction corrected (3) near field method employing the plane wave reciprocity parameter (4).

3. KHIMUNIN A.S. Numerical calculation of the diffraction corrections for the precise measurements of ultrasound absorption. Acustica 27, 173-181, (1972)

4. SIMMONS B.D. and URICK R.J. The plane wave reciprocity parameter and its application to the calibration of electroacoustic transducers at close distances. JASA 21, 633-635, (1949)

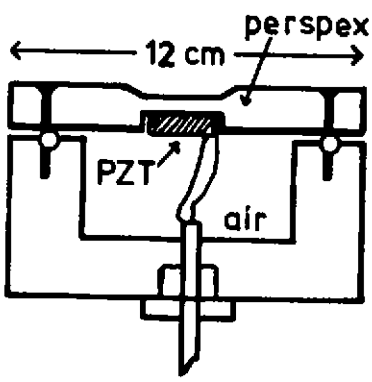

Fig3 Transducer

Face plate thickness	Face plate quarter-wave thickness frequency	Expected position of conductance peaks		Half-power bandwidth of conductance peaks from model		Ratio of spread of expected peak position to bandwidth of the conductance peak	
T mm	f' MHz	$f_1 \pm \Delta f_1$ MHz	$f_2 \pm \Delta f_2$ MHz	$(BW)_1$ MHz	$(BW)_2$ MHz	$\frac{(BW)_1}{2\Delta f_1}$	$\frac{(BW)_2}{2\Delta f_2}$
1.140 ± 0.019	0.588 ± 0.010	0.576 ± 0.013	1.000 ± 0.003	<0.005	0.030	<0.2	5.0
0.866 ± 0.019	0.774 ± 0.017	0.720 ± 0.013	1.040 ± 0.006	0.007	0.036	0.27	3.0
0.815 ± 0.019	0.822 ± 0.020	0.755 ± 0.013	1.057 ± 0.007	0.009	0.039	0.35	2.8
0.741 ± 0.019	0.904 ± 0.023	0.800 ± 0.013	1.090 ± 0.010	0.011	0.020	0.42	1.0
0.717 ± 0.019	0.934 ± 0.025	0.815 ± 0.011	1.104 ± 0.014	0.013	0.018	0.59	0.64
0.628 ± 0.019	1.067 ± 0.032	0.870 ± 0.011	1.185 ± 0.026	0.016	0.014	0.73	0.27
0.512 ± 0.019	1.309 ± 0.050	0.915 ± 0.004	1.370 ± 0.040	0.032	<0.005	4.00	<0.06

Table 1

Face plate quarter-wave thickness frequency	Losses obtained from		1/G' ohms	Efficiency %		
	Conductance peak closest to f_0' for air loading	Fitting model and experimental conductance for water loading		using L_1	using L_2	self-reciprocity
	L_1 ohms	L_2 ohms		η_1	η_2	η_3
0.588 ± 0.010	9.9	9.0	22.2	55	59	
0.774 ± 0.017	12.1	14.0	44.0	73	68	69
0.822 ± 0.020	16.1	16.0	52.0	69	69	78
0.904 ± 0.023	28.9	11.0	57.0	49	80	82
0.934 ± 0.025	28.2	9.0	58.0	51	84	
1.067 ± 0.032	25.8	7.0	50.0	48	86	80
1.309 ± 0.050	14.4	9.0	38.5	63	77	76

Table 2

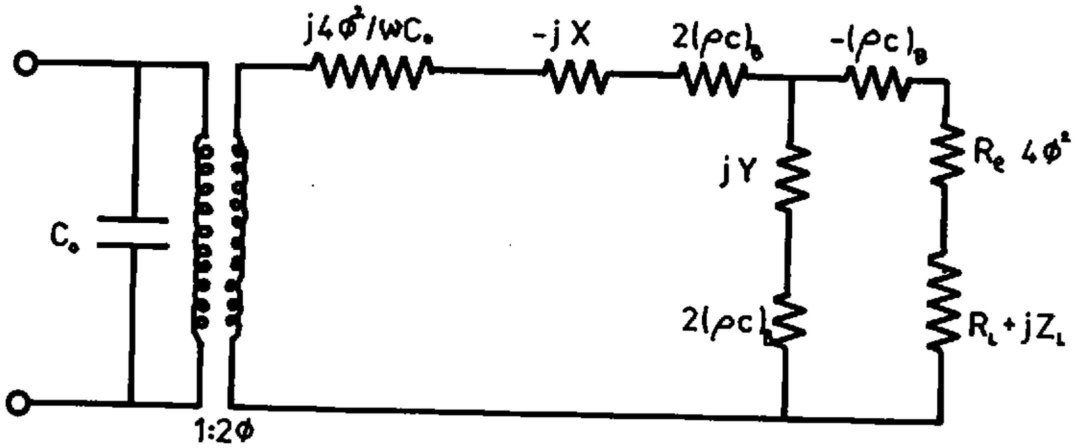

$X=2A(\rho c)_c \cot \alpha_0$

$Y=2A(\rho c)_c \tan \alpha_0$

$B=(\rho c)_B$

$$R_L=\frac{A(\rho c)^2_{FP}(\rho c)_{load}(1+\tan^2\alpha')}{(\rho c)^2_{FP}+(\rho c)^2_{load}\tan^2\alpha'}$$

$$Z_L=\frac{A(\rho c)_{FP}((\rho c)^2_{FP}-(\rho c)^2_{load})\tan\alpha'}{(\rho c)^2_{FP}+(\rho c)^2_{load}\tan^2\alpha'}$$

Specific acoustic impedances are denoted by (ρc) where for
(a) the backing= $(\rho c)_B$ =420kg/m²s
(b) the ceramic= $(\rho c)_c$ =33.7*10↑6kg/m²s
(c) the face plate= $(\rho c)_{FP}$ =3.16*10↑6kg/m²s
(d) the load= $(\rho c)_{load}$ =1.48*10↑6kg/m²s; water
(e) the load= $(\rho c)_{load}$ =420kg/m²s; air
area=A=4.91*10↑-4m²
ceramic thickness freq=f_0 =1.11MHz
$f_0'=f_0(1-2\phi^2/(A(\rho c)_c\pi^2 f_0 C_0))$=0.9925MHz
transformer voltage ratio ϕ=4.061
face plate quarter-wave thickness freq=f'
static capacitance=C_0=1.72*10↑(-9)F
electrical losses=R_e ohms
$\alpha'=(\pi/2)f/f'$; $\alpha_0=(\pi/2)f/f_0$

FIGURE 1 EQUIVALENT CIRCUIT OF TRANSDUCER

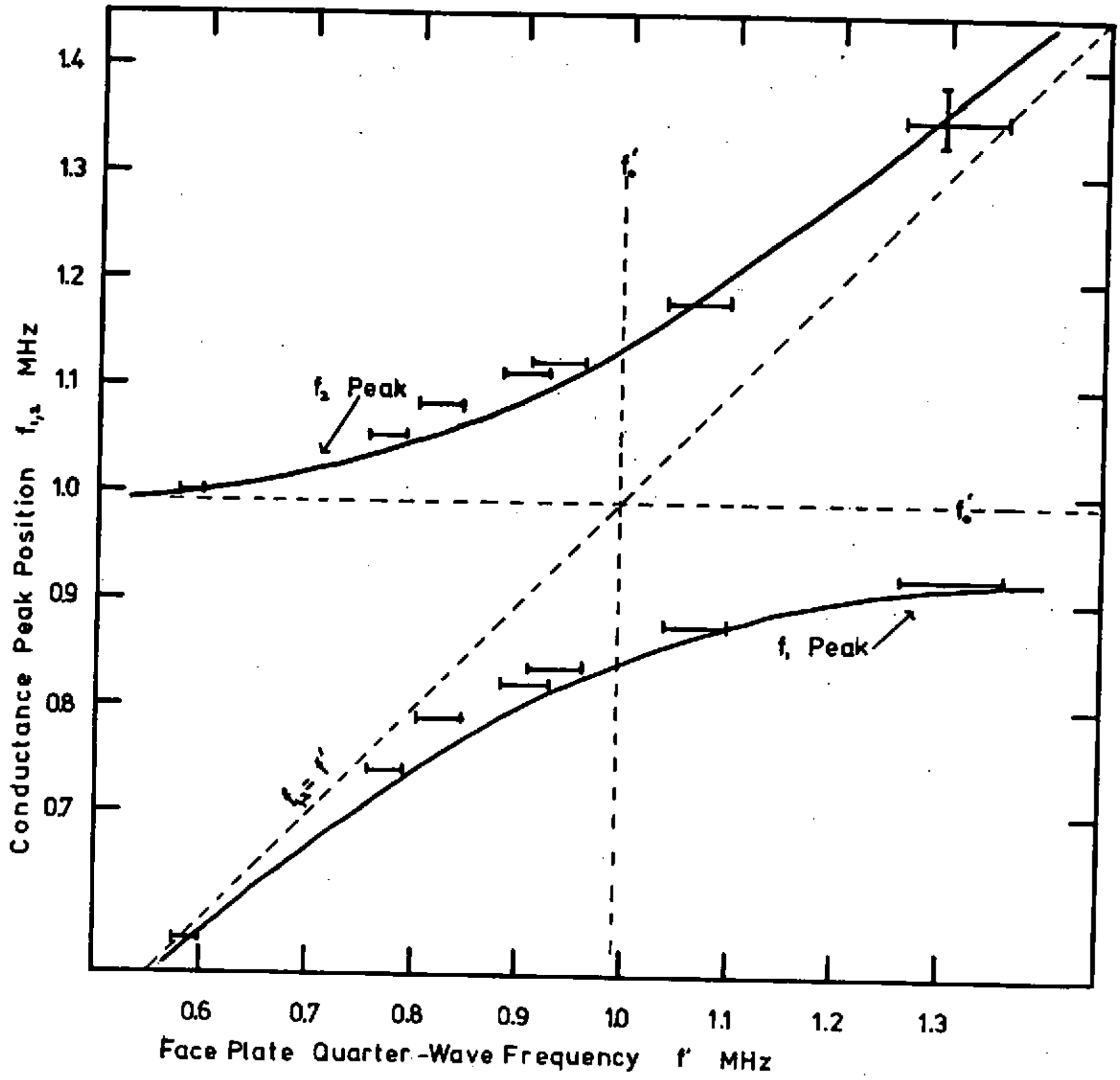

FIGURE 2 Variation of the positon of the two peaks in the input conductance for air loading with face plate quarter-wave frequency. The solid line is predicted by the model. The experimentally determined peak positionsare shown with their error bars

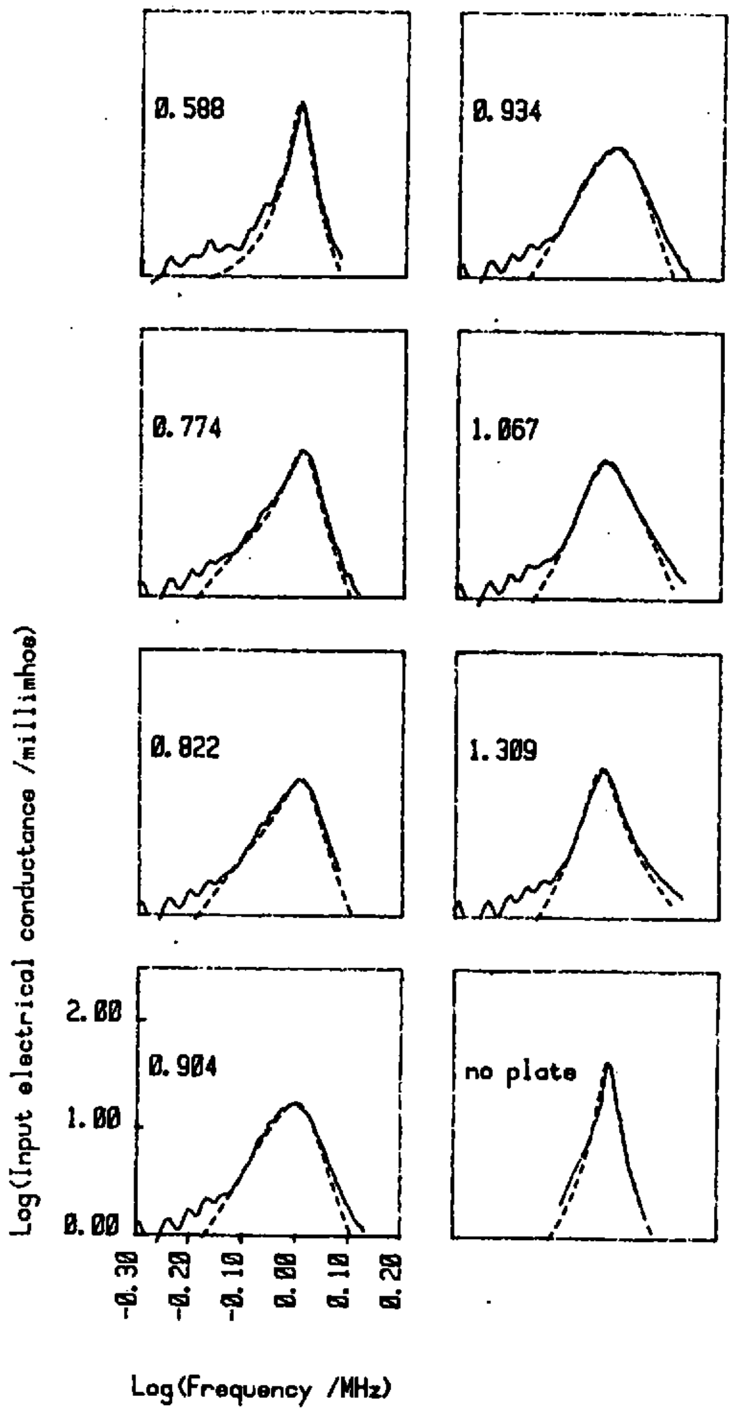

FIGURE 4a Input electrical conductance of transducers with water loading, as predicted by the model (-----) and as measured (———). The face plate quarter-wave frequency is indicated for each case in MHz

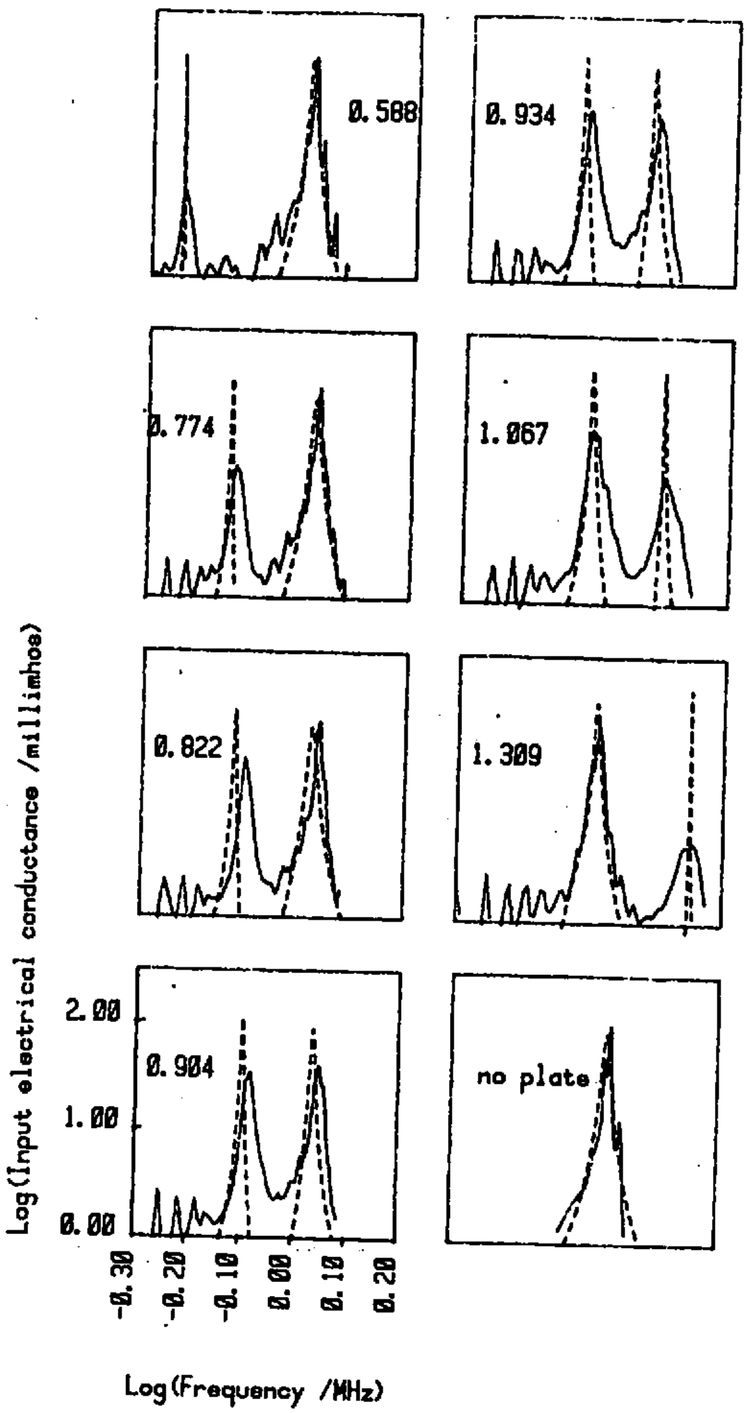

FIGURE 4b Input electrical conductance of transducers with air loading, as predicted by the model (----) and as measured (——). The face plate quarter-wave frequency is indicated for each case in MHz

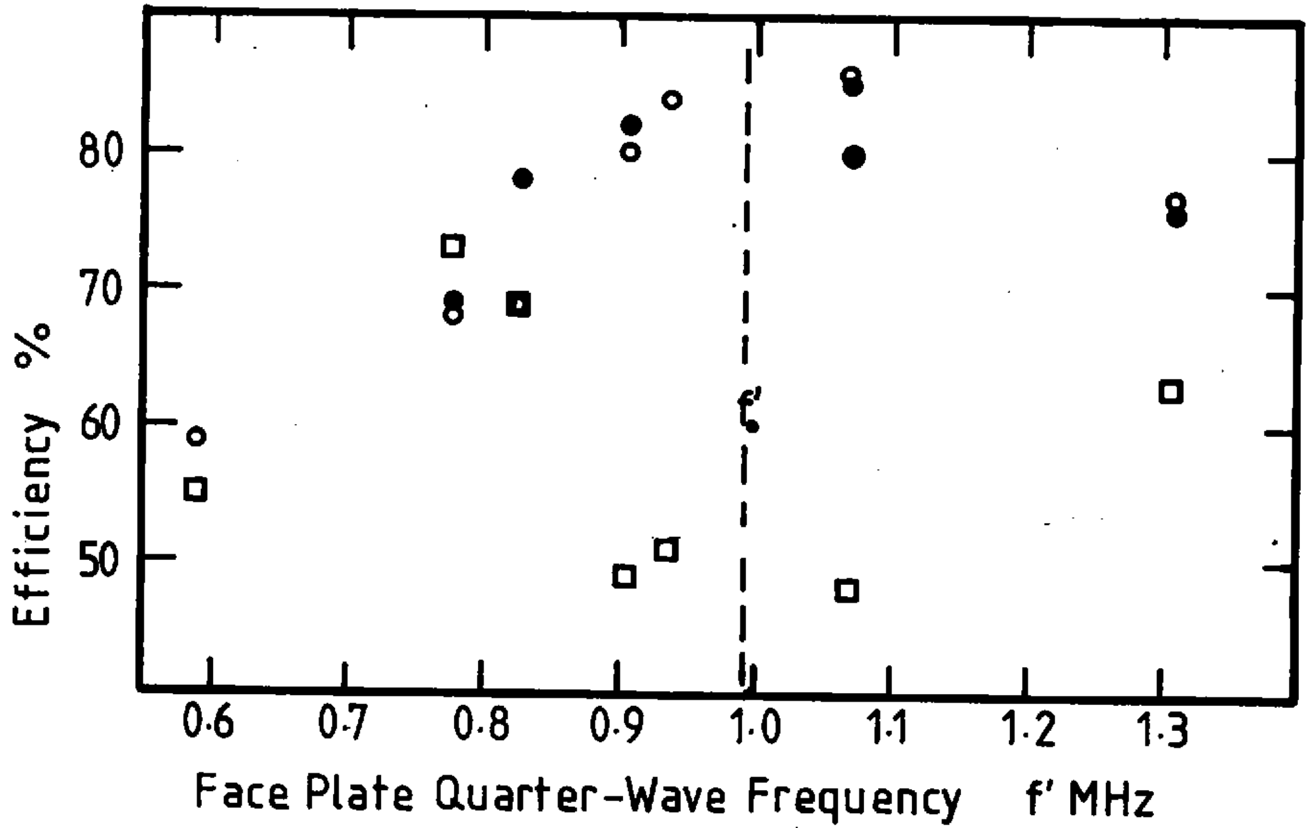

FIGURE 5 Estimates of the transducer efficiency

● Self-reciprocity method

□ using losses L_1

○ using losses L_2